SCIENCE CHINA
Chemistry

•ARTICLES•

February 2021 Vol.64 No.2: 253–262
https://doi.org/10.1007/s11426-020-9874-6

The mechanodonor-acceptor coupling (MDAC) approach for uni-directional multi-state fluorochromism

Luyan Gu[1†], Lujia Zhang[2†], Xiao Luo[4*], Ying Zheng[6], Zhiwei Ye[6], Meng Lv[3], Jinquan Chen[3], Chunlai Chen[2*], Yi Xiao[6], Weihong Zhu[1,5], Xuhong Qian[1] & Youjun Yang[1*]

[1]*State Key Laboratory of Bioreactor Engineering, Shanghai Key Laboratory of Chemical Biology, School of Pharmacy, East China University of Science and Technology, Shanghai 200237, China;*
[2]*School of Life Sciences; Beijing Advanced Innovation Center for Structural Biology; Beijing Frontier Research Center for Biological Structure, Tsinghua University, Beijing 100084, China;*
[3]*State Key Laboratory of Precision Spectroscopy, East China Normal University, Shanghai 200062, China;*
[4]*School of Chemistry and Molecular Engineering, East China Normal University, Shanghai 200241, China;*
[5]*School of Chemistry and Molecular Engineering, East China University of Science and Technology, Shanghai 200237, China;*
[6]*State Key Laboratory of Fine Chemicals, Dalian University of Technology, Dalian 116024, China*

Received August 17, 2020; accepted September 14, 2020; published online December 28, 2020

Uni-directional multi-state fluorochromic scaffolds are valuable photofunctional molecules and yet scarce. We report a general approach for their design, *i.e.*, mechanodonor-acceptor coupling (MDAC). A photochromic molecule is a mechanodonor, due to its capability to convert photonic energy into mechanical force. Upon proper coupling, it can be used to drive a mechanochromic molecule for uni-directional multi-state fluorochromism. The embodiment of this approach is a rhodamine-dithienylethylene hydride (RDH), which has been successfully employed in super-resolution localization microscopy

mechanodonor-acceptor coupling, fluorochromism, diarylethene-rhodamine hybrid, single-molecule imaging

Citation: Gu L, Zhang L, Luo X, Zheng Y, Ye Z, Lv M, Chen J, Chen C, Xiao Y, Zhu W, Qian X, Yang Y. The mechanodonor-acceptor coupling (MDAC) approach for uni-directional multi-state fluorochromism. *Sci China Chem*, 2021, 64: 253–262, https://doi.org/10.1007/s11426-020-9874-6

1 Introduction

Photochromic materials [1] exhibiting photo-triggered switching between two or more spectrally distinct states are the cornerstones of a wide-variety of cutting-edge applications, *e.g.*, spatiotemporally controlled drug-release [2], diffraction-unlimited super-resolution microscopy [3], photopharmacology [4], molecular logic gates [5], and molecular motors/machines [6]. Classic examples are azobenzene, diarylethene, spiropyran, fulgide, and chromene [7]. Recent years have also witnessed the emergence of many novel binary photochromic scaffolds, such as the acylhydrazones [8], azo-BF_2 switches [9], NHC-chelate dimesitylboron [10], a NIR-light operated dihydropyrene [11], imidazolyl based systems [12], dibenzobarrlenes [13], heterodiazocines [14], Stenhouse adducts [15], hydroazulenes [16], hemithioindigo [17], and AIEgen systems [18]. All these aforementioned ones are two-state photochromes (A→B→A). Recently, a paradigm shift from these binary to ternary or even higher-order molecular systems is ongoing because of their capability to exponentially expand the attainable information space in molecular logic gates and functional complexities in optomechanical systems. Though multi-state fluorochromes are not rare feats, design of uni-directional multi-state systems remains challenging.

†These authors contributed equally to this work.
*Corresponding authors (email: youjunyang@ecust.edu.cn; chunlai@tsinghua.edu.cn; xluo@chem.ecnu.edu.cn)

Multi-state fluorochromic systems have been routinely constructed with two or more ($n \geq 2$) binary photochromic molecules [19]. Typically, the photochromic units are orthogonal and therefore can be switched independently. For applications in optomechanics, unidirectional switching of a multi-state system, *e.g.*, a four-state system operating in way of A→B→C→D→A, is required [20]. This could theoretically be constructed with two engaging photochromic scaffolds, *i.e.*, the photoswitching of one enabling/disabling the switching of the other. Engaging mechanism can be electronic [3a], or steric [5g] in the existing systems. It is our interest to develop a rational approach allowing systematic design of such unidirectional multistate systems, *via* a mechanic engaging mechanism. We argue that a photochromophore can be regarded as a photo-induced mechanodonor, because photochromism inevitably triggers a concomitant structural alteration, which has been elegantly exploited as the mechanistic basis of molecular machines and photopharmacology (Figure 1). Upon proper mechanodonor-acceptor coupling (MDAC), such a mechanodonor could be harnessed as a trigger of a second mechanoacceptor to furnish multi-state fluorochromes. The mechanodonor is a fluorochrome responsible for converting the light energy into molecular motion or intramolecular strain, which is then exploited to activate the mechanochemistry [21] of a second mechanochromphore, *i.e.*, mechanoacceptor.

In this work, we report a novel multi-state fluorochrome (**RDH**) following the MDAC approach. Structurally, **RDH** is a hybrid of a dithienylethene and a rhodamine lactone, which are engaged to each other *via* a five-membered spiro-lactone ring. Photo-triggered unidirectional four-state fluorochromic properties were evaluated. Colorimetrically, these four forms adopt either colorless or magenta-colored states. Fluorometrically, they may adopt one of the three different states, *i.e.*, dark, weak and strong. Excited-state dynamics were studied and their three-state fluorescence signals were confirmed by single-molecule spectroscopy. Potentials for localization microscopy were verified.

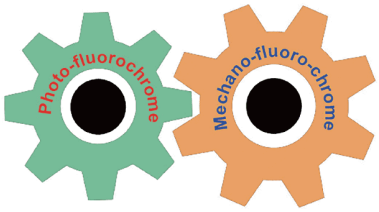

Figure 1 The MDAC to access unidirectional multi-state fluorochromism (color online).

2 Experimental

2.1 Materials and instruments

All the starting materials were obtained from commercial suppliers and used as received. Details are in the Supporting Information online.

2.2 Synthesis and characterization

*2.2.1 Synthesis of 3,4-dibromo-1-methyl-1H-pyrrole-2,5-dione (**3** [22])*

3,4-Dibromo-1*H*-pyrrole-2,5-dione (2.5 g, 1 equiv., 9.81 mmol) was dissolved in 30 mL of MeCN, and methyl *p*-toluenesulfonate (5.48 g, 3 equiv., 29.43 mmol) and NaH (259 mg, 1.1 equiv., 10.79 mmol) was added. The mixture was stirred at 80 °C for 10 h before 1 mL H_2O was added into the solution. The dissolvent was removed under reduced pressure. A saturated solution of NH_4Cl (50 mL) was added and the resulting mixture was extracted repeatedly with dichloromethane. The organic layer was combined, dried with $MgSO_4$ and filtered. The solvent was removed by evaporation and the residue was purified by silica gel column chromatography (petroleum ether and EtOAc (50:1, *v*/*v*)) to give 1.65 g of compound **3** in a 63% yield as a white solid. ^{1}H NMR (400 MHz, $CDCl_3$): δ 3.13 (s, 3H).

*2.2.2 Synthesis of (2,5-dimethylthiophen-3-yl)boronic acid (**4** [23])*

3-Bromo-2,5-dimethylthiophene (2 g, 1 equiv., 10.47 mmol) was dissolved in 40 mL anhydrous tetrahydrofuran (THF). *n*-Butyllithium (2.5 M in hexane, 6.28 mL, 1.1 equiv., 11.51 mmol) was slowly added at −78 °C, and the reaction solution was stirred at the same temperature for 15 min. A solution of tri-*n*-butyl borate (3.09 mL, 1.1 equiv., 11.51 mmol) in THF (10 mL) was added over a period of 10 min. The reaction solution was slowly heated to room temperature and stirred for 8 h. Then 9 mL 2 M HCl was added and the mixture was stirred for another 10 h. After the reaction was completed, the excess solvent was removed and NaOH solution was added to neutralize. The resulting mixture was extracted with dichloromethane and water for three times before the combined organic phases were dried over $MgSO_4$ and the solvent was removed to obtain a crude product. The crude product was dissolved in 15 mL of dichloromethane and washed three times with 2 M NaOH solution. The resulting aqueous phases were combined and 10 mL concentrated hydrochloric acid (12 M) was added dropwise to commence the precipitation of **4** in a 73% yield as a white powder (1.2 g). ^{1}H NMR (400 MHz, $CDCl_3$): δ 7.07 (s, 1H), 2.82 (s, 3H), 2.46 (s, 3H).

*2.2.3 Synthesis of 3,4-bis(2,5-dimethylthiophen-3-yl)-1-met-hyl-1H-pyrrole-2,5-dione (**5** [24])*

Compound **3** (600 mg, 1 equiv., 2.23 mmol) and compound **4** (765.84 mg, 2.2 equiv., 4.91 mmol) were dissolved in dioxane (50 mL), and then CsF (257.86 mg, 4 equiv., 8.93 mmol)

was added. This solution was bubbled with Ar for 15 min. Then $Pd(PPh_3)_4$ (1.67 g, 0.1 equiv., 0.22 mmol) was added. The solution was once again bubbled with Ar for 15 min, heated to 90 °C and stirred for 10 h before cooled to room temperature. The dissolvent was removed under reduced pressure. A saturated solution of Na_2CO_3 (30 mL) was added to the solution and the mixture was extracted with dichloromethane for three times. The organic layer was combined, dried over $MgSO_4$ and filtered. The solvent was removed by evaporation and the residue was purified by silica gel column chromatography (petroleum ether and EtOAc (40:1, *v*/*v*)) to give 325 mg of compound **5** in a 44% yield as a yellow solid. ^{1}H NMR (400 MHz, $CDCl_3$): δ 6.71 (s, 2H), 3.11 (s, 3H), 2.41 (s, 6H), 1.86 (s, 6H).

*2.2.4 Synthesis of 3,4-bis(2,5-dimethylthiophen-3-yl)furan-2,5-dione (**1** [25])*

Compound **5** (225 mg, 1 equiv., 0.679 mmol) was dissolved in 10% KOH aqueous solution (20 mL). The reaction mixture was heated to 100 °C and maintained for 10 h before cooled to room temperature. The product was then obtained by adding 2 M HCl to commence the precipitation of 3,4-bis(2,5-dimethylthiophen-3-yl)furan-2,5-dione (**1**, 201 mg) in a 93% yield as a light yellow powder. ^{1}H NMR (400 MHz, $CDCl_3$): δ 6.75 (d, *J*=0.9 Hz, 2H), 2.42 (s, 6H), 1.92 (s, 6H).

*2.2.5 Synthesis of 3′,6′-bis(diethylamino)-3,4-bis(2,5-dimethyl-thiophen-3-yl)-5H-spiro[furan-2,9′-xanthen]-5-one (**RDH**)*

3,3′-Oxybis(4-bromo-*N*,*N*-diethylaniline) (589.28 mg, 1.5 equiv., 1.25 mmol) was dissolved in 40 mL anhydrous THF. Then *n*-butyllithium (2.5 M in hexane, 1 mL, 3 equiv., 2.51 mmol) was slowly added at −78 °C, and the reaction solution was stirred at the same temperature for 15 min to yielded **6**, A solution of compound **1** (266 mg, 1 equiv., 0.83 mmol) in anhydrous THF (10 mL) was added over a period of 10 min. The reaction solution was slowly heated to room temperature and stirred for 8 h. Saturated NH_4Cl solution was added to the reaction flask, and the mixture was extracted with dichloromethane for three times. The organic layer was combined, dried over $MgSO_4$ and filtered. The solvent was removed by evaporation and the residue was purified by silica gel column chromatography (petroleum ether and EtOAc (20:1, *v*/*v*)) to give 262 mg of **RDH** in a 51% yield as a light red solid. ^{1}H NMR (400 MHz, $CDCl_3$): δ 7.10 (d, *J*=8.9 Hz, 2H), 6.80 (d, *J*=0.9 Hz, 1H), 6.45 (dd, *J*=8.9, 2.6 Hz, 2H), 6.36 (d, *J*=2.5 Hz, 2H), 5.71 (d, *J*=0.9 Hz, 1H), 3.37 (dd, *J*=7.1, 2.2 Hz, 8H), 2.42 (s, 3H), 2.13 (s, 3H), 1.97 (s, 3H), 1.73 (s, 3H), 1.18 (t, *J*=7.1 Hz, 12H). ^{13}C NMR (151 MHz, $CDCl_3$): δ 172.2, 158.4, 152.9, 149.6, 138.2, 136.6, 136.3, 136.2, 129.3, 127.8, 127.7, 126.7, 124.2, 124.0, 108.3, 104.1, 98.1, 44.5, 15.4, 15.3, 14.6, 14.5, 12.7. ESI-HRMS (*m*/*z*): $[M+H]^+$ calcd. for $C_{36}H_{41}N_2O_3S_2$, 613.2559; found 613.2558.

2.2.6 Synthesis of 3,5-dibromo-2-methylthiophene (7 [26])

2-Methylthiophene (5 g, 1 equiv., 50.93 mmol) was dissolved in 50 mL glacial acetic acid solution and then *N*-bromosuccinimide (NBS) (18.13 g, 2 equiv., 101.87 mmol) was slowly added to the solution at room temperature. After stirring for 1.5 h, the reaction solution was poured into ice water and saturated Na_2CO_3 solution was added to neutralize. The resulting mixture was extracted with dichloromethane and the organic layer was dried over $MgSO_4$ and concentrated. The obtained crude product was separated by silica gel column chromatography (petroleum ether) to give 11.50 g of compound **7** in an 88% yield as a colorless liquid. ^{1}H NMR (400 MHz, $CDCl_3$): δ 6.85 (s, 1H), 2.34 (s, 3H).

*2.2.7 Synthesis of 3-bromo-5-(4-methoxyphenyl)-2-methyl-thiophene (**8** [26])*

$Pd(PPh_3)_4$ (316 mg, 0.01 equiv., 0.273 mmol) and (4-methoxyphenyl)boronic acid (3.27 g, 1.1 equiv., 21.49 mmol) was added to a stirred THF solution (120 mL) of **7** (5 g, 1 equiv., 19.53 mmol). 2 M aqueous Na_2CO_3 (60 mL) was delivered to the reaction mixture, which was heated at 80 °C under an argon atmosphere. After 10 h, the solution was cooled down to room temperature and poured into water. The organic layer was extracted with dichloromethane, dried over anhydrous $MgSO_4$ and concentrated. The residue was purified by silica gel column chromatography (dichloromethane and methanol (50:1, *v*/*v*)), to give 4.2 g of compound **8** in a 76% yield as a beige solid. ^{1}H NMR (400 MHz, $CDCl_3$): δ 7.43 (d, *J*=8.9 Hz, 2H), 6.98 (s, 1H), 6.90 (d, *J*=8.9 Hz, 2H), 3.83 (s, 3H), 2.40 (s, 3H).

*2.2.8 Synthesis of (5-(4-methoxyphenyl)-2-methylthiophen-3-yl)boronic acid (**9** [27])*

Compound **8** (4.2 g, 1 equiv., 14.83 mmol) was dissolved in 40 mL anhydrous THF. *n*-Butyllithium (2.5 M in hexane, 8.9 mL, 1.5 equiv., 22.25 mmol) was slowly added at −78 °C, and the reaction solution was stirred at the same temperature. After 15 min, a solution of tri-*n*-butyl borate (6 mL, 1.5 equiv., 22.25 mmol) in THF (10 mL) was added over a period of 10 min. The reaction solution was slowly heated to room temperature and stirred for 8 h. Then 9 mL 2 M HCl was added and the reaction solution was stirred for another 10 h. After the reaction is complete, saturated NaOH solution was added, and the resulting mixture was extracted with dichloromethane and water. After three extractions, the combined organic phases are dried over anhydrous $MgSO_4$ and the solvent was removed to obtain a crude product. The crude product was dissolved in 15 mL of dichloromethane and washed three times with 2 M NaOH solution. The resulting aqueous phases were combined and 10 mL con-

centrated hydrochloric acid (12 M) was added dropwise to commence the precipitation of **9** (3.0 g) in an 82% yield as a white solid. ^{1}H NMR (400 MHz, $(CD_3)_2SO$): δ 7.46–7.43 (m, 3H), 6.96 (d, *J*=8.8 Hz, 2H), 3.77 (s, 3H), 2.58 (s, 3H).

*2.2.9 Synthesis of 3,4-bis(5-(4-methoxyphenyl)-2-methylthiop-hen-3-yl)-1-methyl-1H-pyrrole-2,5-dione (**10**)*

Compound **3** (600 mg, 1 equiv., 2.23 mmol) and compound **9** (1.38 g, 2.5 equiv., 5.58 mmol) were dissolved in dioxane (50 mL), and CsF (1.36 g, 4 equiv., 8.93 mmol) was added. This solution was bubbled with Ar for 15 min. Then $Pd(PPh_3)_4$ (257.86 mg, 0.1 equiv., 0.22 mmol) was added. The solution was once again bubbled with Ar for 15 min, heated to 90 °C and stirred for 10 h before cooled to room temperature. The dissolvent was removed under reduced pressure. A saturated solution of Na_2CO_3 (30 mL) was added to the solution and the mixture was extracted with dichloromethane for three times. The organic layer was combined, dried over $MgSO_4$ and filtered. The solvent was removed by evaporation and the residue was purified by silica gel column chromatography (petroleum ether and EtOAc (15:1, *v/v*)) to give 410 mg of compound **10** in a 34% yield as a yellow solid. ^{1}H NMR (400 MHz, $CDCl_3$): δ 7.47 (d, *J*=8.8 Hz, 4H), 7.19 (s, 2H), 6.90 (d, *J*=8.8 Hz, 4H), 3.82 (s, 6H), 3.17 (s, 3H), 2.01 (s, 6H). ^{13}C NMR (151 MHz, $CDCl_3$): δ 171.0, 159.4, 141.3, 140.2, 133.2, 127.8, 127.0, 126.6, 123.2, 114.4, 55.4, 24.4, 15.1. ESI-HRMS (*m/z*): $[M+Na]^+$ calcd. for $C_{29}H_{25}NO_4S_2Na$, 538.1123; found 538.1122.

*2.2.10 Synthesis of 3,4-bis(5-(4-methoxyphenyl)-2-methylthiophen-3-yl)furan-2,5-dione (**11**)*

Compound **10** (200 mg, 1 equiv., 0.387 mmol) was dissolved in 10% KOH aqueous solution (20 mL). The reaction mixture was heated to 100 °C, maintained for 10 h before cooled to room temperature. The product was then obtained by adding 2 M HCl to commence the precipitation of compound **11** (175 mg) in a 90% yield as a blackish green powder. ^{1}H NMR (600 MHz, $CDCl_3$): δ 7.47–7.45 (m, 4H), 7.20 (s, 2H), 6.92–6.90 (m, 4H), 3.83 (s, 6H), 2.07 (s, 6H). ^{13}C NMR (151 MHz, $CDCl_3$): δ 165.0, 159.7, 142.2, 142.1, 134.6, 127.1, 126.6, 126.2, 122.6, 114.5, 55.5, 15.3. ESI-HRMS (*m/z*): $[M+Na]^+$ calcd. for $C_{28}H_{22}O_5S_2Na$, 525.0806; found 525.0805.

*2.2.11 Synthesis of 3′,6′-bis(diethylamino)-3,4-bis(5-(4-metho-xyphenyl)-2-methylthiophen-3-yl)-5H-spiro[furan-2,9′-xanthen]-5-one (**12**)*

Compound **6** was prepared in 40 mL anhydrous THF and cooled downed to −78 °C. A solution of compound **11** (200 mg, 1 equiv., 0.40 mmol) in THF (10 mL) was added over a period of 10 min. The reaction solution was slowly heated to room temperature and stirred for 8 h. Saturated NH_4Cl solution was added to the reaction flask, and the mixture was extracted with dichloromethane for three times. The organic layer was combined, dried over $MgSO_4$ and filtered. The solvent was removed by evaporation and the residue was purified by silica gel column chromatography (petroleum ether and EtOAc (5:1, *v/v*)) to give 150 mg of compound **12** in a 47% yield as a light blue solid. ^{1}H NMR (600 MHz, $CDCl_3$): δ 7.48 (d, *J*=8.8 Hz, 2H), 7.24 (s, 1H), 7.17 (d, *J*=8.9 Hz, 2H), 7.13 (d, *J*=8.8 Hz, 2H), 6.89 (d, *J*=8.8 Hz, 2H), 6.76 (d, *J*=8.8 Hz, 2H), 6.51 (dd, *J*=8.9, 2.6 Hz, 2H), 6.37 (d, *J*=2.5 Hz, 2H), 6.08 (s, 1H), 3.82 (s, 3H), 3.78 (s, 3H), 3.38 (dd, *J*=9.3, 7.2 Hz, 8H), 2.10 (s, 3H), 1.81 (s, 3H), 1.20 (t, *J*=7.1 Hz, 12H). ^{13}C NMR (151 MHz, $CDCl_3$): δ 172.3, 159.5, 159.2, 159.1, 153.0, 149.6, 140.8, 140.5, 139.1, 137.7, 130.3, 128.7, 127.7, 127.2, 127.0, 126.9, 126.6, 123.6, 123.2, 121.2, 114.3, 114.2, 108.4, 103.7, 98.2, 84.1, 55.5, 55.5, 44.6, 14.9, 14.5, 12.7. ESI-HRMS (*m/z*): $[M+H]^+$ calcd. for $C_{48}H_{49}N_2O_5S_2$, 797.3083; found 797.3082.

*2.2.12 Synthesis of 3′,6′-bis(diethylamino)-3,4-bis(5-(4-methoxyphenyl)-2-methylthiophen-3-yl)-5H-spiro[furan-2,9′-xanthen]-5-one (**13**)*

Under nitrogen atmosphere, BBr_3 (1 M in CH_2Cl_2, 0.88 mL, 5 equiv., 0.88 mmol) was added dropwise to a stirred solution of compound **12** (140 mg, 0.18 mmol) in anhydrous dichloromethane (20 mL) at 0 °C. After that, the reaction mixture was stirred for 5 h at room temperature. Then, the mixture was poured into ice water and filtered to give a light purple solid **13** (45 mg, 33.3%). The compound was used without further purification. ESI-HRMS (*m/z*): $[M+H]^+$ calcd. for $C_{46}H_{45}N_2O_5S_2$, 769.2770; found 769.2759.

*2.2.13 Synthesis of 3′,6′-bis(diethylamino)-3,4-bis(2-methyl-5-(4-(prop-2-yn-1-yloxy)phenyl)thiophen-3-yl)-5H-spiro[furan-2,9′-xanthen]-5-one (**14**)*

Compound **13** (80 mg, 1 equiv., 0.1 mmol) was dissolved in 30 mL of acetone, and 3-bromoprop-1-yne (62 mg, 5 equiv., 0.52 mmol), Cs_2CO_3 (80 mg, 4 equiv., 0.41 mmol) were added. The mixture was stirred for 9 h at 60 °C. The dissolvent was removed under reduced pressure. A saturated solution of NH_4Cl (50 mL) was added and the resulting mixture was extracted repeatedly with dichloromethane. The organic layer was combined, dried over $MgSO_4$ and filtered. The solvent was removed by evaporation and the residue was purified on silica gel using dichloromethane as the eluent to give 38 mg of compound **16** in a 44% yield as a dark blue solid. ^{1}H NMR (400 MHz, $CDCl_3$): δ 7.51–7.46 (m, 2H), 7.24 (s, 1H), 7.17 (d, *J*=8.9 Hz, 2H), 7.15–7.11 (m, 2H), 6.98–6.94 (m, 2H), 6.84 (d, *J*=8.8 Hz, 2H), 6.50 (dd, *J*=8.9, 2.5 Hz, 2H), 6.37 (d, *J*=2.5 Hz, 2H), 6.08 (s, 1H), 4.68 (dd, *J*=18.9, 2.4 Hz, 4H), 3.38 (dd, *J*=6.9, 5.4 Hz, 8H), 2.52 (d, *J*=10.8 Hz, 2H), 2.10 (s, 3H), 1.80 (s, 3H), 1.19 (t, *J*=7.0 Hz, 12H). ^{13}C NMR (151 MHz, $CDCl_3$): δ 172.2, 159.4, 156.9,

156.8, 152.8, 149.4, 140.5, 140.1, 139.2, 137.8, 130.2, 128.6, 128.0, 127.6, 127.6, 126.8, 126.4, 123.7, 123.0, 121.3, 115.3, 115.2, 108.3, 103.6, 98.1, 84.0, 55.9, 55.9, 44.5, 14.8, 14.4, 12.6. ESI-HRMS (*m/z*): $[M+H]^+$ calcd. for $C_{52}H_{49}N_2O_5S_2$, 845.3083; found 845.3082.

2.3 Single molecule imaging

The fluorophore was covalently attached to a surface-immobilized double stranded DNA using a click reaction between azide and alkyne. The single-molecule imaging experiments were performed at 25 °C using a home-built objective-type. Details of the total internal reflection fluorescent (TIRF) microscope were described before [28] (Figure S14, Supporting Information online).

2.4 Super-resolution imaging (PALM)

HeLa cells were stained with 1 μM **RDH** (10% DMSO) for 5 min and washed with PBS for three times. Imaging was performed in normal culture medium without any additives under 2,000 W/cm^2, 532 nm irradiation and reconstructed from 3,000 frames collected in 30 s. Super-resolution imaging analysis was performed in a Thunder-Storm plugin of Image. Briefly, the raw frames were filtered with difference-of-Gaussians filter to select the single-molecule candidates. Then the point spread function (PSF) of single molecule was fitted with an integrated form of symmetric 2D Gaussian function (Fitting radius: 3.0 pixel) following Maximum likelihood method to estimate the precise location and single-molecule intensity. The localization precision was calculated according to the Thompson formula.

3 Results and discussion

3.1 Design rationale and synthesis

RDH was synthesized *via* a 5-step cascade starting from 3,4-dibromo-*N*-methylmaleimide (**3**) (Figure 2). Suzuki-Miyaura coupling of **3** with a dimethylthiophene boronic acid (**4**) afforded **5** in a 44% yield. Further hydrolysis with 10% KOH at 90 °C, followed by an acid-promoted condensation, gave the anhydride (**1**) in a 93% yield. Treatment of **1** with dilithium reagent (**6**) at −78 °C furnished **RDH** in a 51% yield, following a recent xanthene preparation [29].

The design rationale of **RDH** is shown in Figure 3(c). Expectedly, UV-light irradiation of **RDH** (the resting state) potentially promotes the formation of the B-ring of **RDHcc** *via* an electrocyclic reaction of the dithiopheneetheylene (DTE) moiety. During this process, the two thiophene units are pulled together, which results in an internal strain in the ring A of **RDHcc**, and further promot their ring-opening to generate **RDHoc**. **RDHoc** is expected to exhibit an intense magenta color, which is the signature of the rhodamine core, and yet a weak fluorescence because the close-form of the DTE is a known fluorescence quencher *via* photo-induced electron transfer (PET) [30]. Further green-light triggered ring-opening of the B-ring yields **RDHoo**, whose fluorescence is now fully turned-on. The steric repulsion of the two thiophene units of **RDHoo** further promotes the ring closure of the cyclolactone to complete the unidirectional four-state cycle.

3.2 Spectral studies

The photochromic behavior of **RDH** was evaluated in a series of solvents with varying polarity. Irradiation of the CH_2Cl_2, THF, acetone, MeCN, or DMF solution of **RDH** with LED light of 375 nm (30 mW/cm^2) induced an emergence of a broad absorption band covering a broad range of 500–600 nm with a maximum of 550 nm (Figure S4). The quantum yields of the UV light-promoted ring-closing from **RDH** to **RDHcc**, and green light-promoted ring-opening from **RDHcc**-**RDH** were determined to be 48% and 8% respectively in CH_3CN following the reported methods [31]. Apparently, cyclization of the DTE moiety of **RDH** to **RDHcc** occurred. However, further ring-opening of **RDHcc** was not observed due to the magenta color of rhodamine core did not appear, suggesting that the carboxylate was not a sufficiently good leaving group in these non-protic solvents. Therefore, the solvent was switched to MeOH, which is protic and expected to further stabilize the carboxylate *via* hydrogen-bonding and promote the ring-opening (Figure 4).

Upon UV-irradiation of a RDH solution in MeOH, the magenta color corresponding to the absorption band at 552 nm instantaneously appeared and reached a plateau in 2.33 min (Figure 4(a)). We note that a lower-intensity peak at 355 nm, corresponding to the ring-closed form of the dithiopheneethylene unit, rose concomitantly (the white oval circled region, Figure 4(a1)). The co-existence of the absorption bands at 552 and 355 nm confirmed the generation of **RDHoc** (Figure 4(a)). The fluorescence emission studies provided extra evidence for the formation of **RDHoc** in MeOH upon UV irradiation. Excitation of the solution at 555 nm yielded an emission band at 583 nm with a weak fluorescence quantum yield of 0.006 (Figure 4(b)). This is also in agreement with our expectation that **RDHoc** is not supposed to be highly fluorescent due to PET quenching. Then, the solution was irradiated with a green LED light (50 mW/cm^2) to convert **RDHoc** to the highly fluorescent **RDHoo.** This was indeed the case that the fluorescence emission intensity at 590 nm increased by more than 17 fold (Figure 4(b2)). This phenomenon explicitly proved the formation of **RDHcc**, whose fluorescence quantum yield was estimated to be 0.35. While the emission at 583 nm gradually enhanced (Figure 4(a2)), the absorbance at 552 nm de-

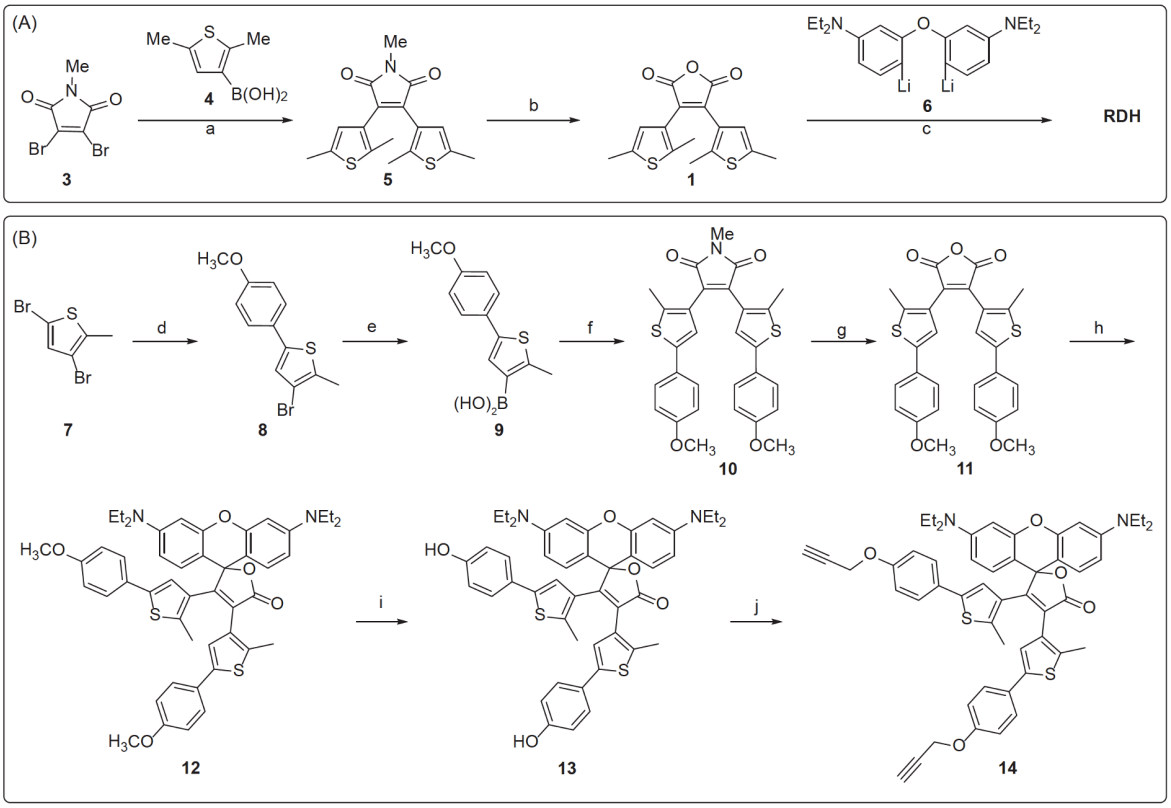

Figure 2 Synthesis of (A) **RDH** and (B) a terminal alkyne substituted **RDH** analogue (**14**). (a) $Pd(PPh_3)_4$, CsF, dioxane, 100 °C, 44%; (b) 1) 10% KOH, 90 °C, 2) 2 M HCl, 93%; (c) THF, −78 °C, 51%; (d) $Pd(PPh_3)_4$, Na_2CO_3, THF/H_2O, 90 °C, 76%; (e) 1) *n*-BuLi, 2) $(nBuO_3)B$, 3) 12 M HCl, 82%; (f) $Pd(PPh_3)_4$, CsF, dioxane, 100 °C, 34%; (g) 1) 10% KOH, 90 °C, 2) 2 M HCl 90%; (h) **6**, *n*-BuLi, THF, −78 °C, 47%; (i) BBr_3, 0 °C, 33%; (j) 3-bromoprop-1-yne, Cs_2CO_3, acetone 60 °C, 44%.

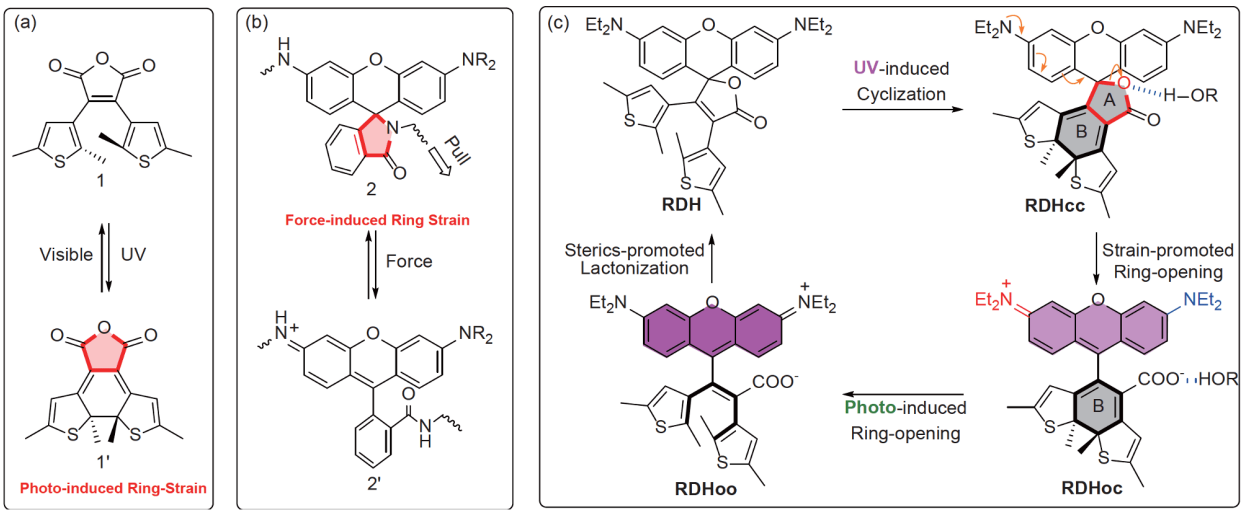

Figure 3 Design rationale of **RDH**. (a) Photo-induced cyclization of dithienylethylene promoted strain in the five-membered anhydride ring. (b) The mechanochemistry of rhodamine lactam. (c) The structure of **RDH** and its photo-triggered unidirectional switching between the four potential forms (color online).

creased (Figure 4(b2)).

This suggested that the ring-closing of **RDHoo** back to **RDH** occurred, which concluded the unidirectional four-state switching of **RDH**. We further showcased that the switching cycle can also be carried out in a mixture of MeOH/H_2O, with the spectral results in 50% MeOH included in Supporting Information online (Figures S2, S3).

The reversible photoswitching of **RDH** was studied (Figure 5). The solution of **RDH** in MeOH was irradiated sequentially with 375 and 520 nm for multiple cycles and the

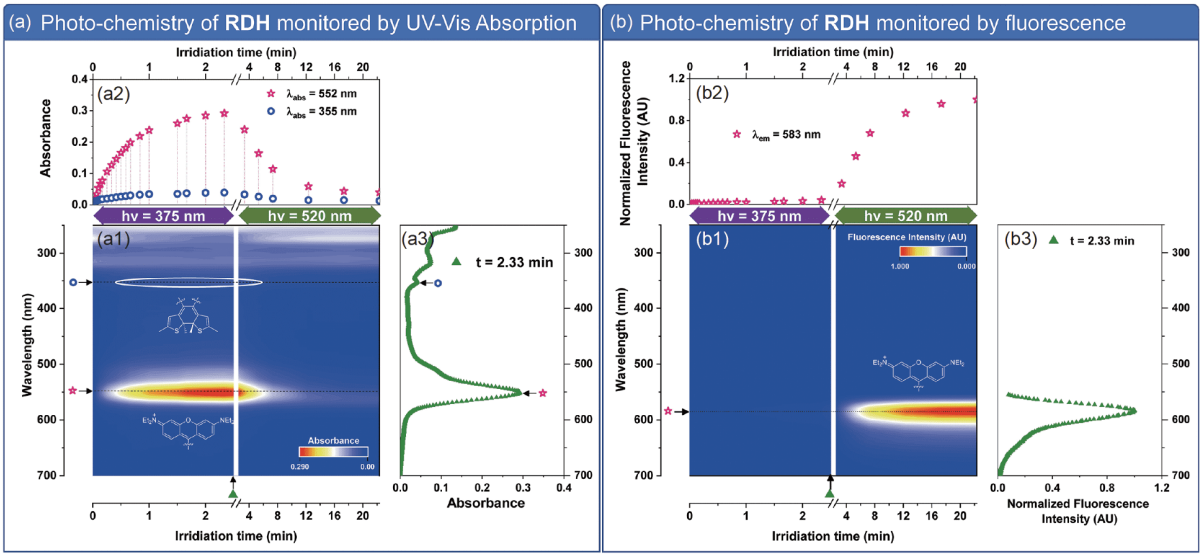

Figure 4 The UV-Vis absorption spectral changes (a) and the fluorescence emission spectral changes (b) of a **RDH** solution (5 μM, in MeOH). (a1) The contour plot of the UV-Vis absorption spectra of a MeOH solution of **RDH** (5 μM) upon UV-irradiation of 375 nm from 0–2.33 min and then green-irradiation of 520 nm from 2.33–22.33 min. (a2) The changes of the absorbance at 355 and 552 nm respectively with respect to the irradiation time. (a3) The UV-Vis absorption spectrum of the solution at 2.33 min. (b1) The contour plot of the fluorescence emission spectra (λ_{ex}=583 nm) of a solution of **RDH** (5 μM) upon UV-irradiation of 375 nm from 0–2.33 min and then green-irradiation of 520 nm from 2.33–22.33 min. (b2) The changes of the emission intensity at 583 nm respectively with respect to the irradiation time. (b3) The fluorescence emission spectrum of the solution at 2.33 min (color online).

fluctuation of both UV-Vis absorbance at 552 nm and the emission intensity at 583 nm was monitored. The general trend was that the extend of the absorbance/emission turn-on at 552 and 583 nm respectively gradually decreased and a background absorbance/emission gradually increases, with respect to the number of cycles (Figures 5(a, b)). This phenomenon suggested a build-up of a previously unexpected substance exhibiting both an absorption at *ca*. 552 nm and a notable emission at *ca.* 583 nm. This substance is not **RHDoo** because it was stable under this condition and not able to spontaneously convert to **RDH** upon sitting. The dithienylethene can go through photo-induced *cis-trans* isomerization if the two thiophene units are not locked in the *cis*-conformation (Figure 5(c)) [32]. Therefore, we propose that this unknown substance is *trans*-**RDHoo**. From reversibility point of view, the formation of *trans*-**RDHoo** is undesired. However, this actually further enriches the already facile photochemistry of **RDH** and can be proved a useful feature in future applications.

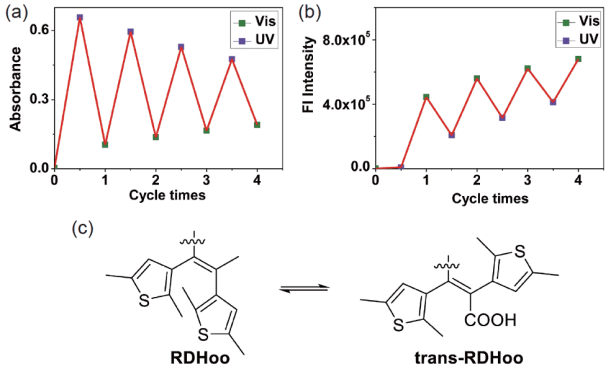

Figure 5 (a) The reversible photoswitching of **RDH** monitored by UV-Vis absorbance at 552 nm. (b) The reversible photoswitching of **RDH** monitored by fluorescence emission intensity at 583 nm with excitation at 550 nm. (c) The *cis-trans* isomerization of dithienylethylene accounting for the reduction of reversibility upon photoirradiation (color online).

3.3 Single molecular imaging of RDH analogue 14

The three-state fluorescence properties, *i.e.* dark-weak-strong, of **RDH** were rare in the literature and therefore, we synthesized a **RDH** analogue **14** which contained alkynyl groups and resorted to single-molecule spectroscopy for confirmation (Figure 6). The fluorophore was covalently attached to a surface-immobilized double stranded DNA with click chemistry (Figure S10). The 405 nm laser-line was used for activation of **14**, and 532 nm was used for excitation of the rhodamine core. Using a TIRF microscope, we captured fluorescence signals produced by individual fluorophore molecules over time. First of all, three-state fluorescence properties were unambiguously observed, which further supported the proposed switching mechanism of **14** (Figure 6(h)). Statistically, the fluorophore stayed in its emissive states for ~1 s, both in aqueous and 50% methanol solutions (Figure S15). And during this period, *ca*. (1.8 −2.3)×10^5 photons were detected, comparable to the photon flux by two bright fluorophores, *i.e.*, Cy3 and TMR (Figures 6(b–g)). Second, we note that different molecules of **14** exhibited interesting heterogeneity under our experimental conditions. While some (*ca*. 33%) events showed multiple

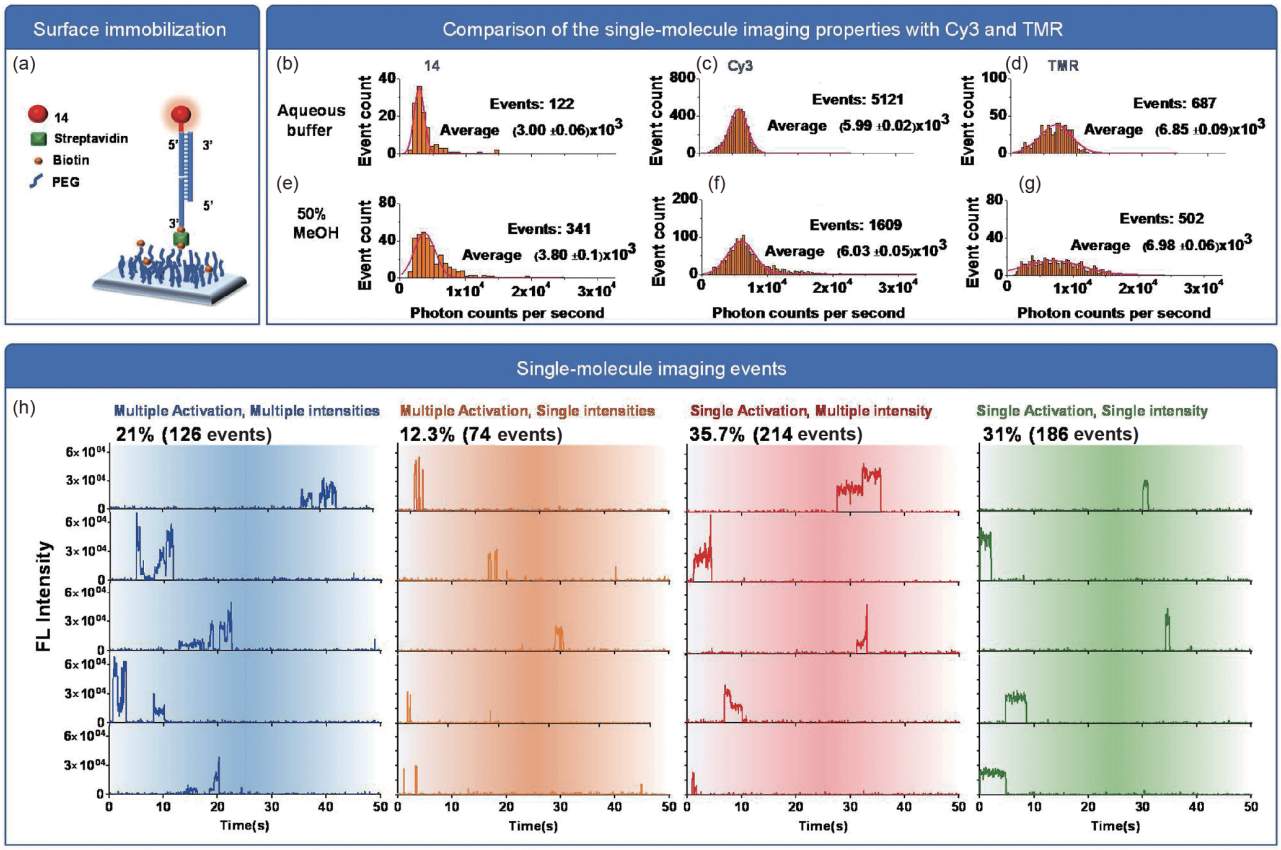

Figure 6 (a) The immobilization approach of **14** onto the surface of PEG-modified glass. (b–d) The histogram of the photon counts per second from each activation event of **14**, Cy3 and TMR, in aqueous phosphate buffer. (e–g) The histogram of the photon counts per second from each activation event of **14**, Cy3 and TMR, in aqueous phosphate buffer containing 50% MeOH. (h) Typical single-molecule fluorescence trajectories of events displayed multiple emission cycles with variable intensities within each emission cycle (blue); of events displayed multiple emission cycles with stable intensities (orange); of events displayed a single emission cycle with variable intensities (red); and of events displayed a single emission cycle with a stable intensity (green) (color online).

off-on cycles, other events were switched on once and was then probably bleached due to the high intensity of laser used in this study. While some exhibited the expected dark-weak-strong profile (Figure 6(h), blue and red), a large fraction exhibited two-state, *i.e.*, OFF-ON emission profile (Figure 6 (h), orange and green). However, this did not necessarily contradict our proposed mechanism since the molecule could spend flitting time on either **14oc** or **14oo** state and render the corresponding "weak" or "strong" state undetected. Also, it was seen that the molecule under investigation was turned on to the "strong" state first and then transited back to the "weak" state, suggesting the UV-triggered conversion of **14oo** to the **14oc** was also viable.

3.4 Potentials of RDH in PALM imaging

Traditionally, the resolution of light microscopy is diffraction-limited [3b]. Namely, the two fluorophores within the distance of *ca*. $\lambda/2$ cannot be distinguished under epi-illumination. In 2006, super-resolution microscopic methods were reported based on single-molecule localization microscopy [33]. Basically, the two fluorophores in close proximity were stochastically photo-activated to allow independent localization of each fluorophore. Therefore, photo-triggered reversible switching or irreversible activation is a prerequisite for a fluorophore to be feasible for localization based microscopy. The off-on switching of the fluorescence properties of **RDH** renders it feasible for photo-activated localization microscopy. The biocompatibility of RDH was verified by a cytotoxicity study with CCK8 kit and the cell viability was found to be higher than 85% (Figure S17). In a proof-of-concept microscopic study, photo-activation of RDH in HeLa cells was tested. Prior to activation, the cells were dark as expected (Figure 7(a)). Upon irradiation of cells with 365 nm (2.4 mW/cm^2) laser line for 60 s, fluorescence of the rhodamine dye at 590 nm upon excitation at 559 nm was observed (Figure 7(b)). This delineated the potentials of RDH for PALM imaging applications. Colocalization studies confirmed that RDH was mito-specific (Figure S16). Therefore, diffraction-unlimited mitochondrial images were obtained, with a localization precision of 22.7 nm. A side-by-side comparison with the

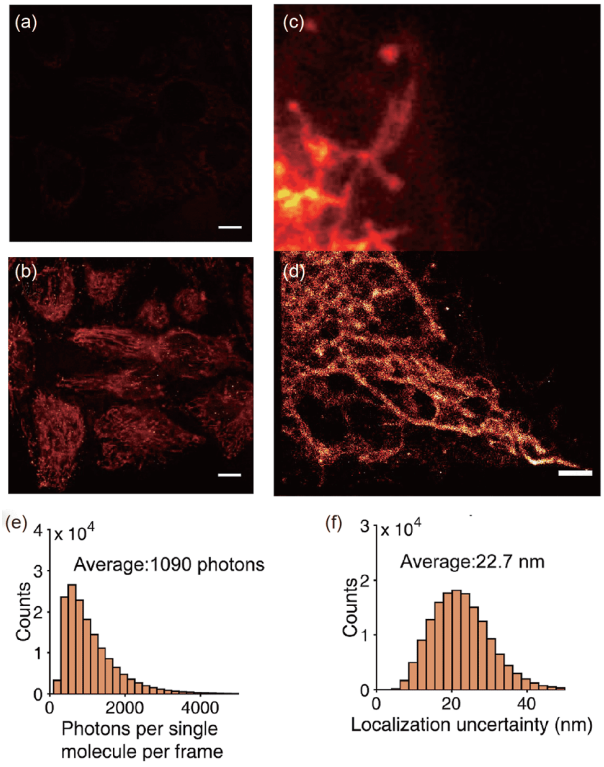

Figure 7 The confocal fluorescence image (a) of HeLa cells incubated with **RDH** (1 μM), with λ_{ex}=559 nm, and λ_{em}=570–630 nm, and the image (b) upon UV-irradiation at 365 nm for 60 s, scale bar: 10 μm. A conventional image (c) of mitochondria and super-resolution image (d) of mitochondria in a live HeLa cell. The histogram of the emitted photons (e) and the localization precision (f) of different photo-triggered activation events, scale bar: 2 μm (color online).

confocal image clearly exhibits the power of PALM in detailing the cell structures (Figure 6(c, d)).

4 Conclusions

We proposed a novel approach for rational design of unidirectional, multi-state fluorochromic systems, *i.e.*, MDAC approach. The embodiment showcased in this manuscript was a rhodamine-DTE hybrid, (**RDH**). It can exist in five different molecular isoforms, *i.e.*, **RDH**, **RDHcc**, **RDHoc**, **RDHoo**, and *trans*-**RDHoo**. Though the formation of *trans*-**RDHoo** is generally not desired since it compromised the fatigue resistance of **RDH**. It could be inhibited through further molecular engineering. Traditional DTE-type photochromic scaffolds were rarely useful for super-resolution localization microscopy because both the ring-open and the ring-closed isomers were non-fluorescent. Such novel photochromic molecules have potentials for super-resolution localization microscopic applications. The MDAC approach presented in this manuscript represents a novel paradigm for the design of fluorophores for localization microscopy, by engaging the robust photo-switching capability of classic photochromic scaffolds with the bright fluorescence of classic fluorochromic scaffolds.

Acknowledgements This work was supported by the National Natural Science Foundation of China (21822805, 21922704, 21877069, 21908065, 22078098), China Postdoctoral Science Foundation (2019M651427, 2020T130197) and the Commission of Science and Technology of Shanghai Municipality (18430711000).

Conflict of interest The authors declare no conflict of interest.

Supporting information The supporting information is available online at http://chem.scichina.com and http://link.springer.com/journal/11426. The supporting materials are published as submitted, without typesetting or editing. The responsibility for scientific accuracy and content remains entirely with the authors.

1 Bamfield P. *Chromic Phenomena: Technological Applications of Colour Chemistry.* Cambridge: RSC, 2001
2 Singh A, Amiji MM. *Stimuli-responsive Drug Delivery Systems.* Cambridge: RSC, 2018
3 (a) Xi H, Zhang Z, Zhang W, Li M, Lian C, Luo Q, Tian H, Zhu WH. *J Am Chem Soc*, 2019, 141: 18467–18474; (b) Uno K, Bossi ML, Irie M, Belov VN, Hell SW. *J Am Chem Soc*, 2019, 141: 16471–16478; (c) Roubinet B, Weber M, Shojaei H, Bates M, Bossi ML, Belov VN, Irie M, Hell SW. *J Am Chem Soc*, 2017, 139: 6611–6620
4 (a) Hüll K, Morstein J, Trauner D. *Chem Rev*, 2018, 118: 10710–10747; (b) Fuchter MJ. *J Med Chem*, 2020, 63: 11436–11447; (c) Morstein J, Dacheux MA, Norman DD, Shemet A, Donthamsetti PC, Citir M, Frank JA, Schultz C, Isacoff EY, Parrill AL, Tigyi GJ, Trauner D. *J Am Chem Soc*, 2020, 142: 10612–10616; (d) Borowiak M, Küllmer F, Gegenfurtner F, Peil S, Nasufovic V, Zahler S, Thorn-Seshold O, Trauner D, Arndt HD. *J Am Chem Soc*, 2020, 142: 9240–9249; (e) Cheng B, Morstein J, Ladefoged LK, Maesen JB, Schiøtt B, Sinning S, Trauner D. *ACS Chem Neurosci*, 2020, 11: 1231–1237; (f) Tian T, Song Y, Wang J, Fu B, He Z, Xu X, Li A, Zhou X, Wang S, Zhou X. *J Am Chem Soc*, 2016, 138: 955–961; (g) Velema WA, Szymanski W, Feringa BL. *J Am Chem Soc*, 2014, 136: 2178–2191
5 (a) Silva APD. *Molecular Logic-based Computation. Cambridge*: RSC, 2012; (b) Erbas-Cakmak S, Kolemen S, Sedgwick AC, Gunnlaugsson T, James TD, Yoon J, Akkaya EU. *Chem Soc Rev*, 2018, 47: 2228–2248
6 Feringa BL, Browne WR. *Molecular Switches.* Weinheim: John Wiley & Sons, 2011
7 Ellis GP. *Chromenes. Chromanones, and Chromones*. New York: John Wiley & Sons, 1977
8 (a) Zheng LQ, Yang S, Lan J, Gyr L, Goubert G, Qian H, Aprahamian I, Zenobi R. *J Am Chem Soc*, 2019, 141: 17637–17645; (b) Shao B, Qian H, Li Q, Aprahamian I. *J Am Chem Soc*, 2019, 141: 8364–8371
9 Yang Y, Hughes RP, Aprahamian I. *J Am Chem Soc*, 2014, 136: 13190–13193
10 Rao YL, Chen LD, Mosey NJ, Wang S. *J Am Chem Soc*, 2012, 134: 11026–11034
11 Bellotto S, Chen S, Rentero Rebollo I, Wegner HA, Heinis C. *J Am Chem Soc*, 2014, 136: 5880–5883
12 Yonekawa I, Mutoh K, Kobayashi Y, Abe J. *J Am Chem Soc*, 2018, 140: 1091–1097
13 Sajimon MC, Ramaiah D, Suresh CH, Adam W, Lewis FD, George MV. *J Am Chem Soc*, 2007, 129: 9439–9445
14 Hammerich M, Schütt C, Stähler C, Lentes P, Röhricht F, Höppner R, Herges R. *J Am Chem Soc*, 2016, 138: 13111–13114
15 Hemmer JR, Poelma SO, Treat N, Page ZA, Dolinski ND, Diaz YJ, Tomlinson W, Clark KD, Hooper JP, Hawker C, Read de Alaniz J. *J Am Chem Soc*, 2016, 138: 13960–13966
16 Broman SL, Petersen MÅ, Tortzen CG, Kadziola A, Kilså K, Nielsen

MB. *J Am Chem Soc*, 2010, 132: 9165–9174
17 (a) Zweig JE, Newhouse TR. *J Am Chem Soc*, 2017, 139: 10956–10959; (b) Petermayer C, Dube H. *J Am Chem Soc*, 2018, 140: 13558–13561
18 Wei P, Zhang JX, Zhao Z, Chen Y, He X, Chen M, Gong J, Sung HHY, Williams ID, Lam JWY, Tang BZ. *J Am Chem Soc*, 2018, 140: 1966–1975
19 Tian H, Zhang J. *Photochromic Materials.* Weinheim: John Wiley & Sons, 2016
20 Tylkowski B, Jastrzab R, Skrobanska M. Photo-sensitive complexes based on azobenzene. In: Jastrzab R, Tylkowski B, Eds. *New-Generation Bioinorganic Complexes*. Berlin: De Gruyter, 2016
21 Li J, Nagamani C, Moore JS. *Acc Chem Res*, 2015, 48: 2181–2190
22 Mei X, Wei K, Wen G, Liu Z, Lin Z, Zhou Z, Huang L, Yang E, Ling Q. *Dyes Pigments*, 2016, 133: 345–353
23 Ko CC, Kwok WM, Yam VWW, Phillips DL. *Chem Eur J*, 2006, 12: 5840–5848
24 Elsner C, Cordes T, Dietrich P, Zastrow M, Herzog TT, Ruck-Braun K, Zinth W. *J Phys Chem A*, 2009, 113: 1033–1039
25 Shorunov SV, Krayushkin MM, Stoyanovich FM, Irie M. *Russ J Org Chem*, 2006, 42: 1490–1497
26 Lee S, You Y, Ohkubo K, Fukuzumi S, Nam W. *Org Lett*, 2012, 14: 2238–2241
27 Meng X, Zhu W, Zhang Q, Feng Y, Tan W, Tian H. *J Phys Chem B*, 2008, 112: 15636–15645
28 Peng S, Sun R, Wang W, Chen C. *Angew Chem Int Ed*, 2017, 56: 6882–6885
29 (a) Luo X, Qian L, Xiao Y, Tang Y, Zhao Y, Wang X, Gu L, Lei Z, Bao J, Wu J, He T, Hu F, Zheng J, Li H, Zhu W, Shao L, Dong X, Chen D, Qian X, Yang Y. *Nat Commun*, 2019, 10: 258; (b) Grimm JB, Brown TA, Tkachuk AN, Lavis LD. *ACS Cent Sci*, 2017, 3: 975–985; (c) Fischer C, Sparr C. *Angew Chem Int Ed*, 2018, 57: 2436–2440
30 de Silva AP, Gunaratne HQN, Gunnlaugsson T, Huxley AJM, McCoy CP, Rademacher JT, Rice TE. *Chem Rev*, 1997, 97: 1515–1566
31 Fukumoto S, Nakashima T, Kawai T. *Angew Chem Int Ed*, 2011, 50: 1565–1568
32 Erko FG, Berthet J, Patra A, Guillot R, Nakatani K, Métivier R, Delbaere S. *Eur J Org Chem*, 2013, 2013: 7809–7814
33 (a) Betzig E, Patterson GH, Sougrat R, Lindwasser OW, Olenych S, Bonifacino JS, Davidson MW, Lippincott-Schwartz J, Hess HF. *Science*, 2006, 313: 1642–1645; (b) Rust MJ, Bates M, Zhuang X. *Nat Methods*, 2006, 3: 793–796